Kinetic Modeling of Catalytic Cracking of Gas Oil Feedstocks: Reaction and Diffusion Phenomena

Mustafa Al-Sabawi, Jesús A. Atias, and Hugo de Lasa*

Chemical Reactor Engineering Centre, Faculty of Engineering, University of Western Ontario, London, Ontario, Canada N6A 5B9

Catalytic cracking experiments of vacuum gas oil on fluid catalytic cracking (FCC)-type catalysts are carried out in a fluidized bench-scale batch Chemical Reactor Engineering Centre (CREC) riser simulator reactor. These experiments are conducted under operating conditions similar to those of the industrial FCC process in terms of temperature, catalyst-to-oil ratio, partial pressure of reactant and products, and reaction times. The crystallite size of the supported zeolite is varied between 0.4 and 0.9 microns with both activity and selectivity being monitored. A five-lump kinetic model describing the catalytic cracking of vacuum gas oil is considered, which accounts for diffusional constraints experienced by hydrocarbon species while evolving in the zeolite pore network. This study provides insights into the effect of intracrystalline diffusion in the catalytic cracking of heavy feedstocks. Results show that the catalyst with the smaller crystallite size provides higher activity and selectivity for desirable intermediate products (gasoline) and lower selectivity for terminal products (coke).

1. Introduction

The demand for advancement in zeolite science and technology has been persistent over the past 40 years,[1] especially today since refineries need to improve the processing of heavy feedstocks into valuable gasoline and other lighter products while reducing costs. To meet these demands, catalysts used in fluid catalytic cracking (FCC) operations will have to be more active, and in particular, more selective for desirable products.[2]

Commercial fluid catalytic cracking catalysts are typically 60 μm pellets that contain H-USY zeolite crystallites supported on an amorphous matrix.[3] H-USY zeolites are the direct result of a steaming process, where the Y zeolites are hydrothermally treated in order to cause dealumination of the crystallite framework.[4] The steaming process is important because it generates mesopores, which give hydrocarbon molecules access to the Brønsted acid sites located inside the crystallites. Y zeolites have a well-defined lattice structure. Their tetrahedral building blocks have a silicon or aluminum atom at their center and oxygen atoms at the four corners. These tetrahedrons link to form sodalite cages, which in turn form 12.4 Å supercages connected via 7.4 Å windows.

FCC catalyst activity and selectivity can be improved in several ways, one of which is to change the zeolite crystallite size. The addition of a shape-selective molecular sieve and the selection of an active matrix may also improve the function of the catalyst.[5] Although the latter two approaches have been addressed, the focus has been mainly on controlling the zeolite crystallite size because of its influence on the diffusional pathway.[6]

Catalytic cracking reactions of gas oil molecules involve a series of steps, which are highly dependent on the zeolite crystallite size. Upon diffusing through the matrix mesopores, gas oil molecules reaching the external surface of the zeolite crystallites must first diffuse through the zeolite pore structure until they reach the active sites within the crystallites. The molecules will then adsorb on these sites and undergo cracking. Products of catalytic cracking diffuse through the zeolite micropores to the external crystallite surface and, subsequently, through the large matrix channels. Thus, it is apparent from this series of steps that catalytic cracking of gas oil is greatly affected by the diffusion of hydrocarbons through the zeolite pore network.

The amount of coke produced and deposited on the catalyst is an important parameter that, not only affects the catalyst's activity, but also determines the "heat balance" in the reactor−regenerator system.[7] The introduction of heavier feedstocks is becoming a common practice nowadays among the refiners, and as a consequence, this heavier feed stream produces more coke, which may cause the regenerator to operate at unacceptable temperatures. Furthermore, as the cracking reactions develop inside the reactor, the catalyst is progressively deactivated with the formation of coke on its surface, rapidly lowering its activity.[8]

Several kinetic models have been proposed for catalytic cracking of vacuum gas oil, some of which group hydrocarbons according to the chemical species type, while others consider compounds according to their boiling point.[9,10] On this basis, three-, four-, and five-lump models have been reported in the literature, including contributions by Ancheyta-Juárez and co-workers[9,11] and Lee et al.[12] A major issue that is common in each of these models is that they fail to consider the important effects of hydrocarbon diffusion in the catalyst pore network, but instead, describe the combined effect of diffusion and reaction by pseudoparameters. Therefore, these models are not adequate for defining the role of diffusion in fluid catalytic cracking.

In the present study, catalytic experiments of vacuum gas oil on FCC-type catalysts were carried out in a bench-scale batch minifluidized bed reactor. Experiments were conducted under similar operating conditions to those of FCC in terms of temperature, catalyst-to-oil ratio, partial pressure of reactant and products, reaction times, and fluidization regime. The crystallite size of the supported zeolite was varied, and activity and selectivity results were analyzed. A five-lump kinetic model, including gas oil, light cycle oil, gasoline, light gases, and coke, was considered. This model specifically accounts for the

* To whom correspondence should be addressed. Tel.: (519) 661-2144. Fax: (519) 850-2931. E-mail: hdelasa@eng.uwo.ca.

10.1021/ie050683x CCC: $33.50
Published on Web 02/04/2006

diffusional constraints experienced by hydrocarbons in the zeolite pore network, providing new insights into the effect of intracrystalline diffusion in the catalytic cracking of heavy feedstocks.

2. Kinetic Modeling—Diffusion and Reaction Phenomena

The catalytic cracking of vacuum gas oil in the minifluidized Chemical Reactor Engineering Centre (CREC) riser simulator is an unsteady-state reaction process. If chemical reactions are assumed to take place in the zeolite crystallites of the FCC catalyst only, given the chemically inert matrix, a material balance of reactant species i in the outer surface of an assumed spherical zeolite crystallite can be written as

$$-\frac{V}{W_{cr}}\frac{dC_{i,ex}}{dt}=\left\{D_{eff,i}\left.\frac{\partial C_{i,in}}{\partial r}\right|_{r=R_{cr}}\right\}\frac{3}{R_{cr}\rho_{cr}} \quad (1)$$

with $C_{i,ex}$ and $C_{i,in}$ representing the gas oil concentration outside and inside the crystallite, respectively. In eq 1, V represents the volume of the riser simulator, W_{cr} represents the mass of crystallites, ρ_{cr} represents the USY zeolite density, R_{cr} represents the crystallite radius, and D_{eff} represents the effective diffusivity of species i in the USY zeolite pore network.

Modeling of the cracking reaction, as given in eq 1, has to be complemented by a partial differential equation in the assumed spherical zeolite crystallite, as follows,

$$\frac{D_{eff,i}}{r^2}\frac{\partial}{\partial r}\left(r^2\frac{\partial C_{i,in}}{\partial r}\right)=\rho_{cr}(r_i)-(K_i\rho_{cr}+\epsilon)\frac{\partial C_{i,in}}{\partial t} \quad (2)$$

where r_i is the rate of consumption/formation of species i, ϵ is the crystallite voidage, and K_i is the adsorption constant for species i.

Furthermore, a number of initial boundary conditions are required for modeling catalytic cracking of gas oil in the CREC riser simulator: (a) instantaneous vaporization ($t = 0, C_{i,ex} = C_{i,ex}|_{t=0}$); (b) symmetric concentration profiles inside the crystallites ($r = 0$, $\partial C_{i,in}/\partial r = 0$); and (c) negligible transport limitations around the 60 μm particles and inside the inert matrix ($r = R_c, C_{i,in} = C_{i,ex}$). Conditions (a) and (c) can be fully satisfied under the operating conditions of the CREC riser simulator, whereas condition (b) can be validated by the crystallite shape with all three dimensions being of comparable magnitude.[13]

Solving eqs 1 and 2 numerically proves that the accumulation term on the right-hand side of eq 2 is negligible for reactions with reaction times of 3, 5, and 7 s. This consideration was proven to be valid by Al-Khattaf and de Lasa[14] for reaction times >2 s. Thus, under these conditions, a "quasi-steady-state" effectiveness factor, η_{ss}, can be defined as

$$\eta_{ss}=\frac{r_{mean}}{-k_i C_{i,in}^2|_{r=R_{cr}}} \quad (3)$$

where k_i is the intrinsic kinetic constant and r_{mean} is the observed rate of consumption/formation.

The development of kinetic models for the catalytic cracking of vacuum gas oil is essential in the prediction of the behavior of commercial FCC units. Since thousands of molecules are involved in gas oil cracking, a "lumping" strategy is effective, grouping chemical species according to their boiling point. More complicated models for the catalytic cracking of gas oil can be found in the technical literature, such as the single-event kinetic model, which is based on conventional carbocation rules and intrinsic molecular reactivity,[15] and Mobil's group model, which uses more than 3 000 kinetic entities.[16] These models are highly complex, especially because of the need of sophisticated feedstock and product analysis and "a priori" prediction of many parameters with the risk otherwise of leading to model overparametrization.

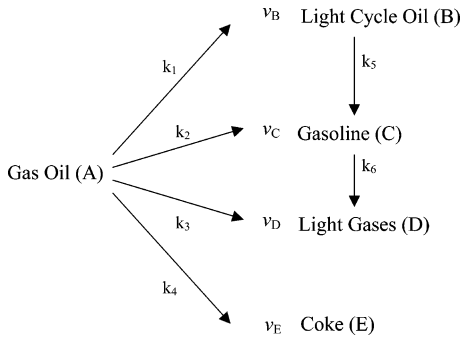

Figure 1. Five-lump reaction network for the catalytic cracking of vacuum gas oil on FCC catalysts.

Table 1. Ranges of Hydrocarbons and Boiling Points for Proposed Lumps

lump	range of hydrocarbons	boiling point range (°C) at 1 atm
light gases	$<C_5$	<36.1
gasoline	C_5-C_{12}	36.1−216.3
light cycle oil	$C_{12}-C_{20}$	216.3−342.7
gas oil	$>C_{20}$	>342.7

The kinetic model of this study considers five lumps (Figure 1): gas oil, light cycle oil (LCO), gasoline, light gases, and coke. These lumps are classified on the basis of boiling point ranges, as reported in Table 1. This model does not account for secondary cracking reactions of products into coke, because kinetic constants for these steps are orders of magnitude smaller than the ones for the primary reactions. Similar approaches are reported by Ancheyta-Juarez et al.[9] and Oliveira and Biscaia.[17]

Thus, under quasi-steady-state conditions and by combining eqs 1−3, the disappearance of gas oil in the well-mixed minifluidized CREC riser simulator can be represented by the following species balance equation,

$$\frac{V}{W_{cr}}\frac{dC_A}{dt}=\eta_{ss}r_A \quad (4)$$

where r_A is the rate of the consumption of vacuum gas oil in the absence of diffusion control and C_A represents the concentration of gas oil in the gas phase.

The proposed model, as given by eqs 2−4, is adequate in the CREC riser simulator considering: (a) the high gas recirculation;[18] (b) the intensively fluidized catalyst securing uniform catalyst activity (constant coke distribution) throughout the bed at a given retention time;[19] (c) the limited thermal cracking with 2−5 wt % conversions at the highest temperature level (570 °C); and (d) the catalytic reaction limited to the zeolite given the inert catalyst matrix used in this study.[3]

Catalytic cracking of gas oil is expected to be strongly affected by gas oil diffusion through the zeolite pore network with the effectiveness factor term, η_{ss}, being an important parameter. On the other hand, the light gases, gasoline, and LCO lump consumptions are not expected to be hindered by diffusion, and therefore, effectiveness factors for these lumps are assumed to be equal to one. This simplification was validated by our research group using model compounds in experiments performed under similar conditions.[13,20,21] For instance, chemical

species with molecule critical diameters in the range of gasoline (e.g., 1,2,4-trimethylbenzene (1,2,4-TMB)) and LCO (e.g., 1,3,5-triisopropylbenzene (1,3,5-TIPB)) are not expected to display diffusional limitations under the temperatures, pressures, and gas-phase concentrations of this study.

The effectiveness factor for the catalytic cracking of vacuum gas can be evaluated by

$$\eta_{ss} = \frac{\tanh(h_i')}{h_i'} \tag{5}$$

where h_i' is a modified Thiele modulus,

$$h_i' = \frac{1}{a_{ext}}\sqrt{\frac{(n+1)}{2}\frac{\rho_{cr}\varphi_{int}k_i C_i^{n-1}}{D_{eff}}} \tag{6}$$

and n is the reaction order (equal to 2 for gas oil cracking), φ_{int} is the catalyst activity decay function, and a_{ext} is the catalyst-specific external surface area.

According to the lumping scheme of Figure 1, the rate of gas oil consumption can be expressed as

$$-\frac{V}{W_{cr}}\frac{dC_A}{dt} = \eta_{ss}\varphi_{int}(k_1+k_2+k_3+k_4){C_A}^2 \tag{7}$$

where k_1, k_2, k_3, and k_4 are the intrinsic rate constants considered in the reaction network of Figure 1. The second order assigned to the gas oil cracking is a frequently adopted assumption given the different reactivity of the various hydrocarbon species forming the gas oil. This matter can be explained by the changing reactivity of the gas oil molecules, where, at low conversions, the most reactive molecules crack more readily and, as the conversion increases, the reactivity of the feed molecules decreases.[10] On the other hand, LCO and gasoline cracking rates, with narrower boiling ranges, can be modeled using first-order reactions, since the kinetic order of cracking single molecules is unity.[22]

The concentration of gas oil, C_A, in the CREC riser simulator, a reactor of constant volume, can be related at any reaction time to the mass fraction, y_A, by

$$C_A = \frac{y_A W_{hc}}{MW_A V} \tag{8}$$

where y_A is the mass fraction of gas oil, W_{hc} is the total mass of hydrocarbons injected in the riser simulator, and MW_A is the molecular weight of gas oil.

Thus, the consumption of gas oil in the riser simulator can be evaluated in terms of mass fractions using the following equation:

$$-\frac{V}{W_{cr}}\frac{dy_A}{dt} = \eta_{ss}\varphi_{int}\left(\frac{W_{hc}}{MW_A V}\right)(k_1+k_2+k_3+k_4){y_A}^2 \tag{9}$$

Furthermore, each intrinsic kinetic constant, k_i, can be postulated to change with the reactor temperature, T, following a reparametrized Arrhenius-type equation,

$$k_i = k_{i0}\exp\left[\frac{-E_i}{R}\left(\frac{1}{T}-\frac{1}{T_0}\right)\right] \tag{10}$$

where E_i represents the energy of activation, k_{i0} is the pre-exponential factor, and T_0 is the centering temperature defined as the average temperature used in the reaction experiments, which is 813 K.

It is well-known that the deposition of coke on the catalyst surface decreases the catalyst activity, since coke covers the active sites of the catalyst. The catalyst activity decay function, φ_{int}, can be accounted for by relating catalyst activity to the coke concentration on the catalyst, as suggested by Froment and Bischoff.[23] Thus, the nonselective catalyst activity decay function φ_{int} can be evaluated by the following expression

$$\varphi_{int} = \exp(-\lambda X_E') \tag{11}$$

where λ is the deactivation parameter for gas oil cracking and X_E' represents the mass of coke produced per mass of gas oil injected.

Similarly, species balances can be established for the other lumps, in terms of both species concentrations and weight fractions, with these balances containing formation and/or consumption of chemical species.

Light Cycle Oil (B):

$$\frac{V}{W_{cr}}\frac{dC_B}{dt} = \varphi_{int}(\nu_B\eta_{ss}k_1{C_A}^2 - k_5 C_B) \tag{12}$$

$$\frac{V}{W_{cr}}\frac{dy_B}{dt} = \varphi_{int}\left[\nu_B\eta_{ss}\left(\frac{W_{hc}}{MW_A V}\right)\left(\frac{MW_B}{MW_A}\right)k_1{y_A}^2 - k_5 y_B\right] \tag{13}$$

Gasoline (C):

$$\frac{V}{W_{cr}}\frac{dC_C}{dt} = \varphi_{int}\left(\nu_C\eta_{ss}k_2{C_A}^2 + \frac{\nu_C}{\nu_B}k_5 C_B - k_6 C_C\right) \tag{14}$$

$$\frac{V}{W_{cr}}\frac{dy_C}{dt} = \varphi_{int}\left[\nu_C\eta_{ss}\left(\frac{W_{hc}}{MW_A V}\right)\left(\frac{MW_C}{MW_A}\right)k_2{y_A}^2 + \frac{\nu_C}{\nu_B}\left(\frac{MW_C}{MW_B}\right)k_5 y_B - k_6 y_C\right] \tag{15}$$

Light Gases (D):

$$\frac{V}{W_{cr}}\frac{dC_D}{dt} = \varphi_{int}\left(\nu_C\eta_{ss}k_3{C_A}^2 + \frac{\nu_D}{\nu_C}k_6 C_C\right) \tag{16}$$

$$\frac{V}{W_{cr}}\frac{dy_D}{dt} = \varphi_{int}\left[\nu_D\eta_{ss}\left(\frac{W_{hc}}{MW_A V}\right)\left(\frac{MW_D}{MW_A}\right)k_3{y_A}^2 + \frac{\nu_D}{\nu_C}\left(\frac{MW_D}{MW_C}\right)k_6 y_C\right] \tag{17}$$

Coke (E):

$$\frac{dX_E}{dt} = \varphi_{int}(\nu_E\eta_{ss}k_4{C_A}^2) \tag{18}$$

$$\frac{V}{W_{cr}}\frac{dX_E'}{dt} = \varphi_{int}\left[\nu_E\eta_{ss}\left(\frac{W_{hc}}{MW_A V}\right)\left(\frac{MW_E}{MW_A}\right)k_4{y_A}^2\right] \tag{19}$$

with ν_i representing the stoichiometric coefficient for lump i and X_E being the mass of coke produced per mass of crystallites. Note that $\sum y_i + X_E' = 1$, and MW_A, MW_B, MW_C, MW_D, and MW_E represent molecular weights for the various lumps, as reported in Table 2.

It is important to note that a_{ext} in eq 6 can be defined using the characteristic dimension of the zeolite crystallite, L, since practically all of the cracking reactions take place in the zeolite

Table 2. Molecular Weights of Various Lumps

lump	molecular weight (kg/kmol)
light gases (C_1-C_4)	46[a]
gasoline (C_5-C_{12})	114[a]
light cycle oil ($C_{12}-C_{20}$)	226[a]
gas oil ($>C_{20}$)	397[b]
coke	800

[a] Evaluated from gas chromatograms. [b] Assessed from thermal experiments.

crystallite with little influence from the matrix of the catalyst.[3] Therefore, approximating the crystallite geometry to an equivalent sphere, $a_{ext} = 6/L$, eq 6 becomes

$$h'_A = \frac{L}{6}\sqrt{\frac{3}{2}\frac{\rho_{cr}\phi_{int}(k_1 + k_2 + k_3 + k_4)C_A}{D_{eff}}} \qquad (20)$$

It is also expected that diffusion of gas oil in a USY zeolite falls under the configurational regime, with this being an activated mechanism whose dependence with temperature can be represented by the Erying equation,[24]

$$D_{eff} = D_0 \exp\left[\frac{-E_D}{R}\left(\frac{1}{T} - \frac{1}{T_0}\right)\right] \qquad (21)$$

where D_0 is the preexponential factor for diffusion and E_D is the activation energy for diffusion.

Although there is extensive work reported on diffusion in zeolites, there is uncertainty on the specific values to be assigned to the effective diffusivities of hydrocarbons under FCC conditions.[25] In this respect, Ruthven and Kaul[26] acknowledge that determined effective diffusivities were obtained in most cases far away from actual FCC process conditions. Thus, it is imperative to assess effective diffusivities under relevant catalytic cracking reaction conditions.

3. Experimental Section—Procedure and Apparatus

Catalytic cracking experiments were performed in a novel Chemical Reactor Engineering Centre (CREC) riser simulator. This laboratory-scale unit, proposed by de Lasa,[19] enables injected gas oil feedstock to vaporize and to come into contact and mix with fluidized catalyst throughout a predetermined time span. The simulator operates isothermally and at constant volume of the reaction mixture. A schematic diagram of this unit and its components can be seen in Figure 2.

The main reactor consists of an upper and lower shell that allows the catalyst to be loaded and unloaded easily into a basket. This basket is located in the lower shell of the reactor. The catalyst basket is bound by two grids, which trap the catalyst and restrict its mobility within the basket. The reactor was designed in such a manner so as to create an annular space between the outer portion of the basket and the inner walls of the bottom shell. This space allows for the recirculation of chemical species in the reactor by the rotation of an impeller positioned above the catalyst basket. A metallic gasket is used to seal the two chambers, and a packing gland assembly with a cooling jacket supports and seals the impeller shaft.

As the impeller rotates, a low-pressure region is formed in the center region of the impeller blades. As a result, gas introduced into the bottom shell of the reactor is induced to flow upward toward this region through the catalyst basket. Upon entering the basket, the gas mixes with the catalyst and causes the solid particles to fluidize, improving the contact

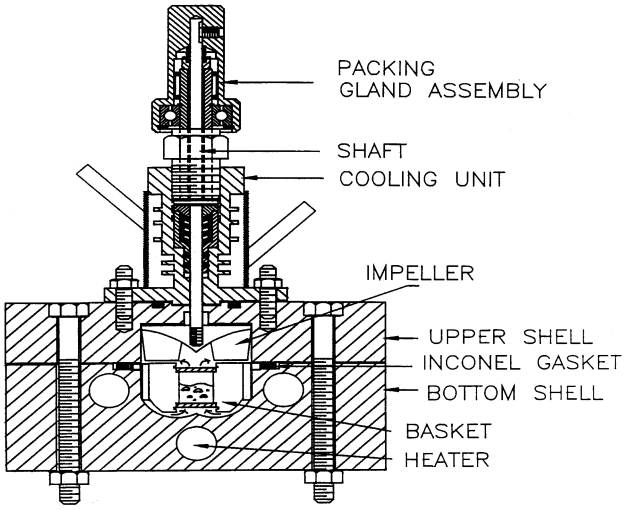

Figure 2. Schematic diagram of the CREC riser simulator.

between the gas and solid phases. Gas mixing patterns in a CREC riser simulator represent a well-mixed unit. Ginsburg et al.[18] reported that gas mixing times corresponding to high recirculation rates in this unit occur over impeller rotational speeds ranging from 3000 to 6000 rpm and total reactor pressures ranging from 1 to 5 atm. The reaction conditions in the riser simulator mimic the cracking conditions in large-scale riser reactors by matching the relative pressures of the chemical species, the gas−solid contact regime temperature, and the reaction time.

The riser simulator operates in conjunction with a series of sampling valves that allow for injection of the gas oil and the withdrawal of reaction products in short periods of time, as shown in Figure 3. A four-port valve enables the connection−isolation of the 54 cm^3 reactor and the 1120 cm^3 vacuum box, and a six-port valve allows for the collection of a sample of reaction products in a sampling loop. Pressure transducers are installed in both the reactor and the vacuum box chambers to monitor the progress of each catalytic cracking experiment.

When the allotted reaction time of a catalytic cracking experiment expires, the four-port valve opens and connects the reactor to the vacuum box, at which point the reactor is evacuated and its products are sent to the vacuum box. This evacuation process occurs instantaneously because of the significant differences in pressure and volume between the reactor and vacuum box. Any further cracking of products present in the vacuum box is abolished because of the low temperature at which the vacuum box is held (340 °C).

The six-port valve with a sampling loop is connected to the vacuum box. This allows for the collection of a sample of the reaction products present in the vacuum box. The collected sample of reaction products is then sent to an Agilent Technologies 6890N gas chromatography (GC) unit to be quantified. The GC unit uses a flame ionization detector (FID) and a HP-1 25 m capillary column of cross-linked methyl silicone with an outer diameter of 0.20 mm and an inner diameter of 0.33 μm. The GC uses a specific temperature program to quantify the reaction products coming from the sampling loop of the riser simulator setup. The column temperature was programmed to be at −30 °C for 3 min, which then increased at a rate of 15 °C/min to 235 °C for 1 min, and finally increased at a rate of 40 °C/min to 320 °C for 4 min. The injector and detector temperatures during the experiments were set to 320 °C. The signals from the GC are quantified by the Chemstation computer software, which generates and displays peaks of different areas and

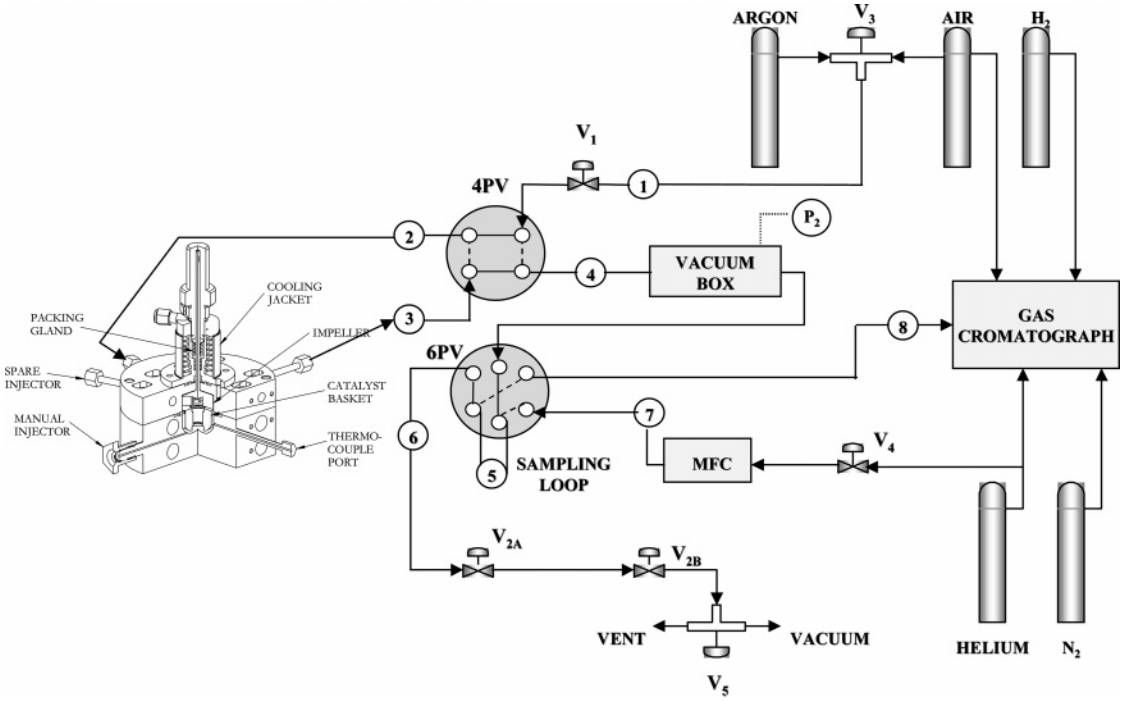

Figure 3. Schematic diagram of the CREC riser simulator experimental set up.

Table 3. Properties of Vacuum Gas Oil Feedstock Used in This Study

property	value
API	21.7
total sulfur, wppm	8700
total nitrogen, wppm	1600
refractive index @ 67 °C	1.4924
aniline point	79.4
carbon residue	0.6
carbon-to-hydrogen ratio	84.7/12.4
viscosity (cSt @ 100 °C)	7.32
simulated distillation	(°C)
initial boiling point (IBP)	211.9
10 wt %	320.3
20 wt %	354.9
30 wt %	382.4
40 wt %	408.0
50 wt %	428.9
60 wt %	449.7
70 wt %	473.7
80 wt %	501.6
90 wt %	536.6
final boiling point (FBP)	632.7

heights, with each peak representing a specific compound. Functions in the Chemstation software allow for the determination of the retention times, area counts, and area percentages per peak.

The reactant injected in the riser simulator was typical vacuum gas oil having a molecular weight of 397 g/mol. This feedstock was obtained from Imperial Oil Limited, located in Sarnia, Ontario, Canada. The analytical data for this feedstock is reported in Table 3.

Two standard FCC catalysts were used in the gas oil catalytic cracking experiments, characterized by Tonetto et al.[3] These two catalysts were prepared following the same procedure, and hence, equivalent acid sites distributions and similar physical properties were attained, with the only exception being the Y-zeolite crystallite size. The catalysts with the larger crystallites (0.9 μm diameter) and the smaller crystallites (0.4 μm diameter) are referred to in this present study as CAT-LC and CAT-SC, respectively.

Table 4. Properties[a] of the FCC Catalysts with Large and Small Crystallite Sizes

	large crystallite CAT-LC	small crystallite CAT-SC
zeolite content[b] (%)	29	31
unit cell size (Å)	24.28	24.28
BET surface area (m^2/g)	197	169
external surface area (m^2/g)	20	25
crystallite size (μm)	0.9	0.4
crystallite density (kg/m^3)	825	825

[a] Properties reported for USY zeolites after being pelletized and exchanged with ammonium nitrate. [b] Comparing area (BET) for zeolites, matrix, and catalysts before steaming.

Given that the only major difference between the two catalysts was the crystallite size, the quantitative evaluation of diffusional constraints could be carried out. The unit cell size was measured by X-ray diffraction following method ASTM D-3942-80, and the surface area was determined using the Brunauer−Emmett−Teller (BET) method. Table 4 summarizes the main properties of both catalysts.

With this end, experiments involving the catalytic cracking of gas oil were carried out at four temperatures of 510, 530, 550, and 570 °C and three reaction times of 3, 5, and 7 s. The catalyst/gas oil ratio was maintained at 5 for each experiment (weight of catalyst = 0.81 g, weight of injected gas oil = 0.162 g). Experiments at each condition were repeated 3−5 times to ensure consistency in results.

4. Catalyst Activity Results—Overall VGO Conversion

An important objective of this study is to analyze the gas oil conversion at typical catalytic cracking conditions using the two catalysts, CAT-LC and CAT-SC. It is observed that the overall gas oil conversion to the lighter lumps increased with both temperature and reaction time. Figures 4 and 5 illustrate this trend for CAT-LC and CAT-SC, respectively. For instance, for the experiments conducted at 5 s using CAT-LC, the gas oil conversions are 40, 55, 63, and 69.5 wt % at temperatures of

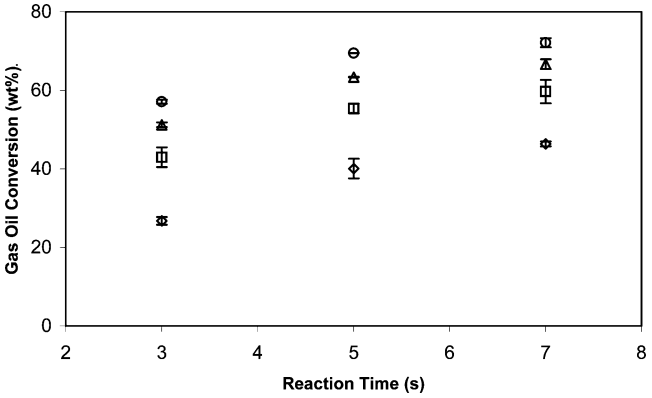

Figure 4. Conversion of vacuum gas oil over CAT-LC at different residence times. Experiments were conducted at temperatures of 510 °C (◊), 530 °C (□), 550 °C (Δ), and 570 °C (○) using a catalyst−gas oil ratio of 5.

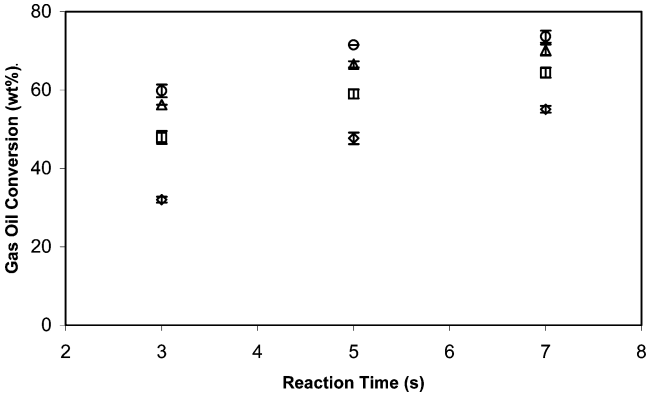

Figure 5. Conversion of vacuum gas oil over CAT-SC at different residence times. Experiments were conducted at temperatures of 510 °C (◊), 530 °C (□), 550 °C (Δ), and 570 °C (○) using a catalyst−gas oil ratio of 5.

510, 530, 550, and 570 °C, respectively. In this respect, the gas oil conversion increases by 15 wt % from 510 to 530 °C, 8 wt % from 530 to 550 °C, and 6.5 wt % from 550 to 570 °C. Similar trends are observed using CAT-SC at the same reaction time, with the gas oil conversions being 48, 59, 66.5, and 71.5 wt % at temperatures of 510, 530, 550, and 570 °C, respectively. Typical errors for the gas oil conversion reached up to ±2.5 wt %. It is observed that increasing the temperature for a given reaction time causes the overall gas oil conversion to significantly rise until a certain level is reached. For instance, it can be noticed that the gas oil conversion, using CAT-SC catalyst, augments significantly from 510 to 530 °C. On the other hand, the increase in conversion between 550 and 570 °C is much milder. On this basis, it is possible to assume that the catalytic cracking reaction under the conditions of the CREC riser simulator displayed an apparent activation energy that changed with temperature, with this activation energy being larger in the lower temperature range and reduced significantly for the higher temperatures. This observation will be further discussed later in this study.

While examining gas oil conversion on USY catalysts, it is apparent that the overall rate of conversion is dependent on pore diffusion resistance within the crystallite network. The gas oil conversions obtained from catalytic cracking runs using the two catalysts, CAT-LC and CAT-SC, were analyzed to determine the influence of internal mass transfer on the calculation of the overall reaction rate. To carry out this analysis, the conversion of gas oil attained using CAT-LC was compared to the conversion obtained using CAT-SC, as shown in Figure 6. In this figure, experimental points that fall on or are close to the

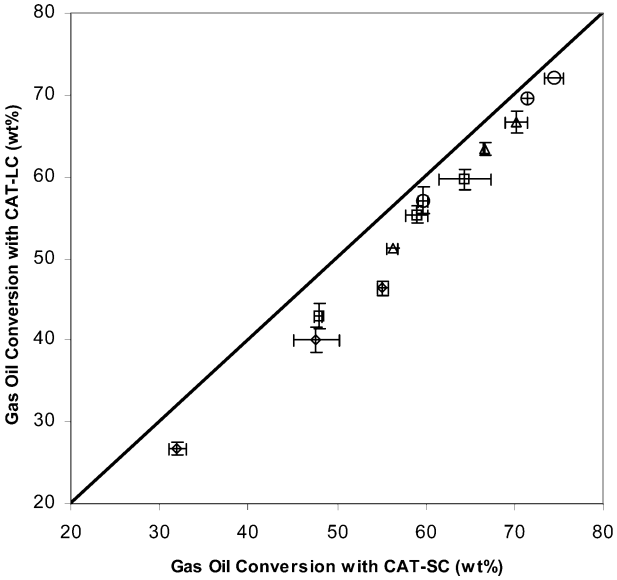

Figure 6. Vacuum gas oil conversion obtained using CAT-LC versus CAT-SC. Experiments were conducted at temperatures of 510 °C (◊), 530 °C (□), 550 °C (Δ), and 570 °C (○) using a catalyst−gas oil ratio of 5. The lowest point of each symbol refers to a reaction time = 3 s, and the middle and highest points refer to 5 and 7 s, respectively.

solid line indicate that CAT-LC and CAT-SC provide similar gas oil conversions, whereas points that are farther away from the solid line denote much higher conversions attained with CAT-SC.

Differences in gas oil conversions between the two catalysts imply that conversion is a strong function of the crystallite size and, therefore, the reaction rate is heavily influenced by intracrystalline diffusion of reactant molecules. On the other hand, similarity in gas oil conversion indicates that the conversion is not significantly affected by the crystallite size and so the reaction rate is less influenced by intracrystalline diffusion. In this respect, it can be noticed that the differences in gas oil conversions using CAT-LC and CAT-SC, which are initially large at lower temperatures and reaction times, become smaller at conditions that correspond to the values of higher conversions (i.e., higher temperatures and residence times). For instance, the gas oil conversions obtained using CAT-LC and CAT-SC at 510 °C and 7 s were 44.5 wt % and 55 wt %, respectively. At 570 °C and 7 s, however, CAT-LC and CAT-SC provided similar conversions, 72 wt % and 73 wt % respectively. The proximity in gas oil conversion, obtained with the two catalysts under specific operating conditions (i.e., higher temperatures of 570 °C), strongly suggests that catalytic cracking of gas oil is less influenced by crystallite size and that diffusion limitations of gas oil molecules in the zeolite pore structure do not play a significant role in influencing the overall catalytic cracking rate. On the other hand, at the lower temperatures (510 °C), one can observe substantial differences between gas oil conversion using CAT-SC and CAT-LC, and these differences are attributed to intracrystallite diffusional effects. It is under these conditions that the intracrystallite diffusion path, along which reactant molecules have to be transported before reaching an active site, becomes a critical parameter.

5. Assessment of Kinetic and Diffusivity Parameters—Five-Lump Model

To evaluate the relative importance of diffusion and reaction phenomena in the catalytic cracking of gas oil, a five-lump model which includes diffusivity coefficients (D_0 and E_D) and

Table 5. Degrees of Freedom for Model Parameter Estimation

	step 1	step 2	
	CAT-LC + CAT-SC	CAT-LC	CAT-SC
no. of indep. pseudospecies data pts	116	62	54
no. of parameters to be estimated	7	8	8
degrees of freedom	109	54	46

kinetic parameters (E_i, k_{i0}, and λ) is considered. Given that the gas oil lump is the only lump whose diffusion through the USY zeolite pore network is potentially hindered under reaction conditions, the five-lump model of this study only takes into account the diffusion coefficients for the gas oil lump.

Parameter calculations involve a two-step process (Table 5). In the first step, kinetic constants associated with primary gas oil cracking reactions into LCO, gasoline, and light gases (k_{10}, k_{20}, $k_{30}E_{10}$, E_{20}, and E_{30}) are combined and represented by two apparent kinetic parameters k'_0 and E'_0 describing the overall primary cracking rate [i.e., $k' = k_1 + k_2 + k_3$, and $k' = k'_0 \exp(-E'_0/RT)$]. These two parameters, along with kinetic parameters involved in the cracking of gas oil into coke (k_{40} and E_{40}), diffusivity parameters (D_0 and E_D), and coke deactivation coefficient (λ) were calculated via nonlinear regression by solving eqs 9, 11, 19, and 21 and using the experimental data points (yields of coke and unconverted gas oil) gathered for both catalysts (CAT-LC and CAT-SC).

The first step of the parameter calculation process involves the evaluation of seven parameters with 109 degrees of freedom (Table 5), making the process of calculating diffusivity parameters under reaction conditions a worthwhile exercise. Resulting parameters are obtained, as reported in Table 6, with low cross-correlation coefficients in most cases, as shown in Table 8. Moreover, as is also shown in Table 7, both D_0 and E_D effective diffusivity parameters are obtained with low 95% confidence intervals.

Upon completing the first step, a second step allows the calculation of kinetic parameters that describe the cracking of gas oil into product lumps such as LCO, gasoline, and light gases. This step involves the evaluation of eight independent kinetic parameters (k_{20}, k_{30}, k_{50}, k_{60}, E_{20}, E_{30}, E_{50}, and E_{60}) for each of the catalysts via nonlinear regression and by solving eqs 15 and 17. The degrees of freedom associated with the calculation of these parameters, as reported in Table 5, are 54 and 46 for CAT-LC and CAT-SC, respectively. Note that k_{10} and E_{10} can be considered as dependent parameters and can be calculated once k_{20}, E_{20}, k_{30}, and E_{30} are determined.

Intrinsic kinetic parameters and diffusivity parameters are reported in Tables 6 and 7, respectively, with their corresponding 95% confidence limits. Differences observed between the fitted kinetic parameters, obtained for both catalysts, are statistically insignificant, and thus, the values of the calculated parameters can be considered to be similar. This consistency in the results is expected since both catalysts have similar acidities and the same structural properties, as shown by Tonetto et al.[3]

The correlation matrices obtained for each of the fittings in steps 1 and 2 show low cross-correlation between most of the fitted parameters (Tables 8 and 9), and this statistically confirms the low level of interaction between the calculated parameters. Furthermore, the 95% confidence limits calculated for each parameter are small (±2−32%), indicating that the fittings obtained are accurate.

In addition, analysis of residual distribution, model-predicted values, and experimental data points for both CAT-LC and CAT-SC catalysts shows a regular distribution of residuals (Figure 7) with no prediction bias, thus proving the adequacy of the proposed kinetic model and the fitted parameters.

It is important to note that the values of the diffusivity parameters (calculated in the first step) were obtained via regression analysis with initial guesses between the following ranges: (a) 42 to 171 kJ for E'_0 and E_4, (b) 0 to 418 kJ for E_D, and (c) the preexponential factors were left unbounded. Initial estimates in these ranges provide small changes in the numerical values of each of the parameters (up to 24% maximum deviation). Initial parameter guesses outside these ample parameter ranges were avoided, given that they lead to a combination of kinetic and effective diffusivity parameters not having proper orders of magnitude.

Since there is very limited information in the technical literature regarding effective diffusivity of gas oil in Y-zeolite catalysts, the values obtained in this study were compared to those predicted by Atias and de Lasa[25] using 1,3,5-triisopropylbenzene (1,3,5-TIPB), a model compound with 15 carbon atoms. These authors reported that the diffusivity of 1,3,5-TIPB at 450 °C was 1.76×10^{-13} m^2/s. This compares favorably with a diffusivity of 0.109×10^{-13} m^2/s calculated for gas oil at the same temperature using the same zeolite and reactor setup. It is important to note that the diffusivity for 1,3,5-TIPB is higher than the diffusivity for gas oil, and this difference can be attributed to the larger size molecules present in the gas oil lump (average carbon number of 28) compared to the 15 carbon atoms in 1,3,5-TIPB.

The difference between the activation energies for the catalytic cracking reaction (83−140 kJ/mol) and for diffusional transport (238 kJ/mol) explains the trends illustrated in Figure 6, with the gas oil conversions obtained using CAT-LC and CAT-SC differing significantly at lower temperatures and becoming close at higher temperatures. At the lower temperatures (up to 530 °C), the mass transport of gas oil molecules

Table 6. Intrinsic Kinetic Parameters for Gas Oil Catalytic Conversion over USY Catalysts

	CAT-LC		CAT-SC	
	value	95% CFL	value	95% CFL
k_{10} ($m^6/(kg_{crystallite}\ mol_{gasoil}\ s)$)	1.172E−02	2.725E−04	1.158E−02	2.465E−04
E_{10} (kJ/mol_{gasoil})	106.32	13.33	97.01	11.54
k_{20} ($m^6/(kg_{crystallite}\ mole_{gasoil}\ s)$)	4.762E−03	1.323E−04	5.036E−03	1.199E−04
E_{20} (kJ/mol_{gasoil})	107.99	5.94	120.61	4.94
k_{30} ($m^6/(kg_{crystallite}\ mole_{gasoil}\ s)$)	4.218E−03	1.402E−04	4.058E−03	1.266E−04
E_{30} (kJ/mol_{gasoil})	122.68	7.39	136.17	6.60
k_{40} ($m^6/(kg_{crystallite}\ mol_{gasoil}\ s)$)	1.493E−03	5.999E−05	1.493E−03	5.999E−05
E_{40} (kJ/mol_{gasoil})	139.65	7.06	139.65	7.06
k_{50} ($m^3/(kg_{crystallite}\ s)$)	5.450E−02	5.604E−03	7.602E−02	4.842E−03
E_{50} (kJ/mol_{LCO})	94.24	22.05	90.43	13.91
k_{60} ($m^3/(kg_{crystallite}\ s)$)	3.236E−02	4.218E−03	4.705E−02	3.907E−03
E_{60} ($kJ/mol_{gasoline}$)	86.24	27.91	82.86	17.90
λ	26.10	1.17	26.10	1.17

Table 7. Diffusivity Parameters for Gas Oil Catalytic Conversion over USY Catalysts

	value	95% CFL
$D_0 \times 10^{13}$ (m^2/s)	9.58	0.34
E_D (kJ/mol)	237.66	6.44

Table 8. Cross-Correlation Matrix for CAT-LC + CAT-SC (Step 1)

	k'_0	E'_0	k_{40}	E_{40}	D_0	E_D	λ
k'_0	1	0.53	0.91	0.29	−0.70	−0.30	0.94
E'_0	0.53	1	0.36	0.93	−0.42	−0.66	0.58
k_{40}	0.91	0.36	1	0.11	−0.63	−0.20	0.73
E_{40}	0.29	0.93	0.11	1	−0.28	−0.57	0.36
D_0	−0.70	−0.42	−0.63	−0.28	1	0.66	−0.57
E_D	−0.30	−0.66	−0.20	−0.57	0.66	1	−0.27
λ	0.94	0.58	0.73	0.36	−0.57	−0.27	1

controls the overall cracking rate. However, given E_D is greater than E'_0, the effect of gas oil molecule transport is quickly promoted with the temperature increase. As a result, the intrinsic chemical reaction becomes the controlling step at 570 °C, with gas oil conversions for CAT-LC and CAT-SC being essentially identical.

Thus, CAT-SC and CAT-LC display, as expected using eqs 5, 6, 9, 10, and 21, relatively different behavior when temperature is increased:

(a) For the low-temperature or diffusional-control regime (510 °C < T < 530 °C),

$$k_i = k_{io} \exp\left(\frac{-E_{app}}{RT}\right) \quad \text{with } E_{app} = \frac{E'_0 + E_D}{2}$$

(b) For the high-temperature regime (550 °C < T < 570 °C),

$$k_i \approx k_{i0} \exp\left(\frac{-E'_0}{RT}\right)$$

This difference of activation energies describes a special feature of the FCC catalyst operation, so-called "diffusion at low temperature−reaction at high temperature" (DLT−RHT) controlled regime, where the highly sensitive thermal mass transfer intracrystalline transport regime dominates lower temperature operation and the less sensitive thermal chemically controlled regime governs at higher temperatures.

Table 9. Cross-Correlation Matrix for CAT-LC (Intrinsic Kinetic Parameters−Step 2)

	k_{20}	E_{20}	k_{30}	E_{30}	k_{50}	E_{50}	k_{60}	E_{60}
k_{20}	1	−0.40	0.15	−0.07	−0.77	0.42	−0.15	0.10
E_{20}	−0.40	1	−0.09	0.19	0.40	−0.77	0.11	−0.20
k_{30}	0.15	−0.09	1	−0.49	−0.70	0.44	−0.97	0.60
E_{30}	−0.07	0.19	−0.49	1	0.40	−0.71	0.55	−0.96
k_{50}	−0.77	0.40	−0.70	0.40	1	−0.66	0.73	−0.50
E_{50}	0.42	−0.77	0.44	−0.71	−0.66	1	−0.51	0.75
k_{60}	−0.15	0.11	−0.97	0.55	0.73	−0.51	1	−0.69
E_{60}	0.10	−0.20	0.60	−0.96	−0.50	0.75	−0.69	1

6. Catalyst Selectivity Results−Yields of Products

Once the various kinetic and diffusion parameters were determined, the distributions of the four product lumps (LCO, gasoline, light gases, and coke) were calculated by solving the set of eqs 13, 15, 17, and 19 with the 13 kinetic and 2 transport parameters as determined in Section 5.

Figures 8 and 9 illustrate the lump distributions as a function of the gas oil conversion. Vertical lines in these figures represent the 3, 5, and 7 s reaction times in the CREC riser simulator. It can be observed that light gases, gasoline, and coke are consistently increasing with reaction time, whereas the LCO yield initially augments with the progression of reaction until it levels off, reaching a maximum. This maximum level of LCO yield can be explained considering the competition between LCO formation reactions and the overcracking of LCO into gasoline.

Comparing the product yields attained at 510 °C with the CAT-LC and CAT-SC, it can be noticed from Figures 8 and 9 that both catalysts display different lump selectivities, especially for the LCO and gasoline intermediate products. For instance, at a reaction time of 7 s, CAT-LC and CAT-SC yielded the following: 17 and 20 wt % of LCO, 14 and 18.3 wt % of gasoline, and 11 and 14 wt % of light gases, respectively.

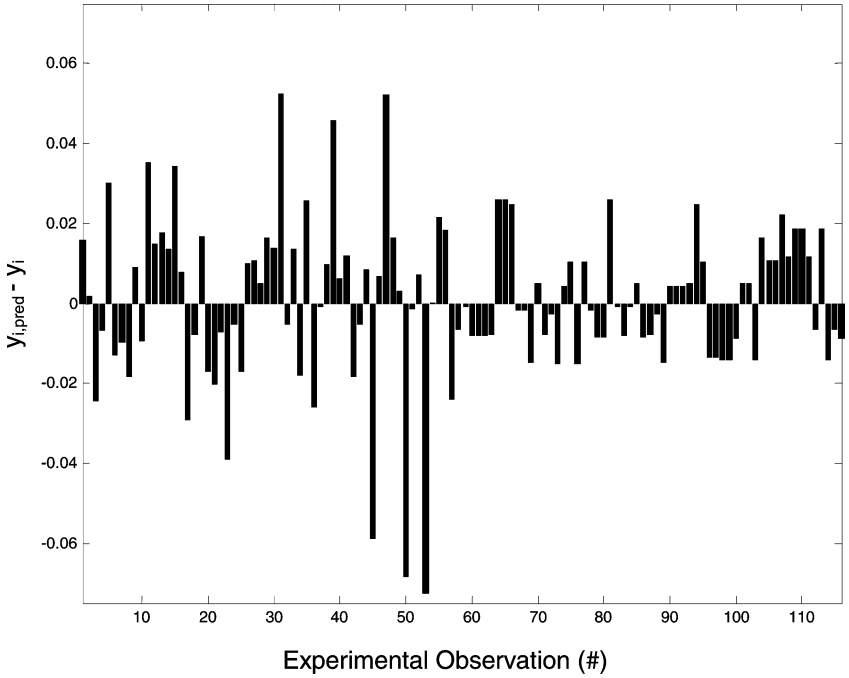

Figure 7. Residual distribution for nonlinear regression of data obtained using CAT-LC and CAT-SC in step 1 of the parameter calculation process.

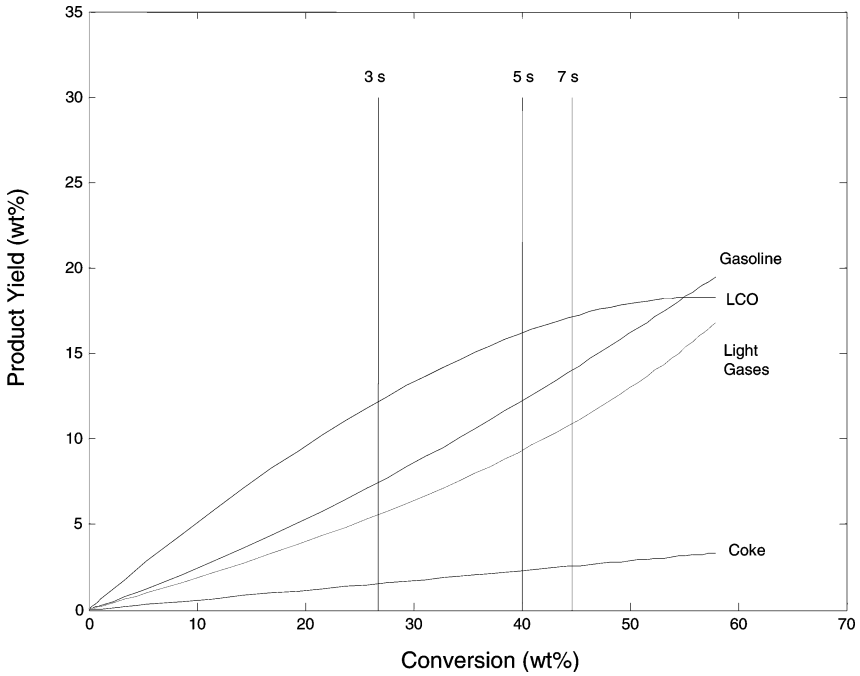

Figure 8. Product selectivity obtained from CAT-LC at a temperature = 510 °C and for a C/O = 5.

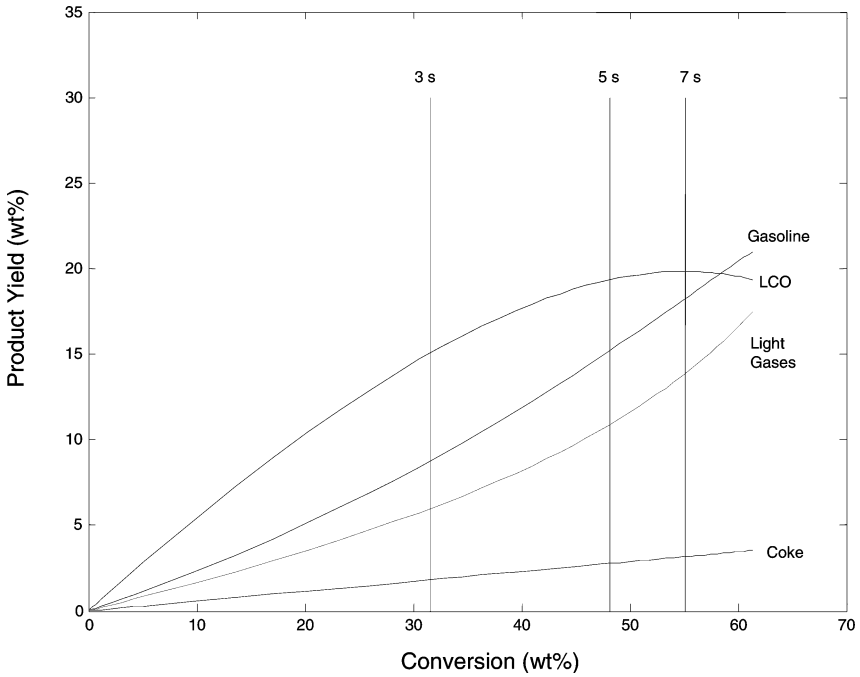

Figure 9. Product selectivity obtained from CAT-SC at a temperature = 510 °C and for a C/O = 5.

It should be stressed that these observed differences are due to the gas oil being catalytically cracked at conditions where diffusion limitations are significant (lower temperatures). As expected, a catalytic cracking process controlled by intracrystalline diffusion of reactant molecules is favored by the reduction of the crystallite size. Smaller crystallite zeolites provide higher accessibility to their active sites with an increased capacity for the cracking of gas oil molecules, leading to higher overall gas oil conversions.

From the previously described results, it can also be observed that not only do the smaller crystallite zeolites (CAT-SC) provide larger overall vacuum gas oil (VGO) conversions than the large crystallite zeolites (CAT-LC) but they also provide higher selectivity of desired products (i.e., gasoline) while reducing the selectivity of undesired product species (i.e., coke). For instance, at 510 °C and 7 s, the CAT-SC and CAT-LC catalysts display a 28.7% and 25.2% selectivity for gasoline, respectively.

Differences in gasoline yields and selectivity between the two catalysts studied can be traced to the net effect of competing reactions: (a) gasoline formation reactions, cracking of both VGO and LCO, and (b) gasoline overcracking reactions. Gasoline formation reactions involve cracking of larger molecules, such as gas oil and LCO, into smaller hydrocarbon molecules, with gas oil cracking being strongly influenced by intracrystalline transport at lower temperatures. On the other hand, gasoline overcracking reactions, which involve relatively smaller gasoline molecules, are uninfluenced by crystallite size.[3]

Thus, with smaller zeolite crystallites (CAT-SC), the gasoline formation reactions are increased while the overcracking reactions remain essentially unaffected, and all of this leads to higher gasoline yields and selectivities. In this respect, gasoline yields obtained in this study are, in the context of their changes with crystallite size, consistent with data reported in the technical literature by Camblor et al.,[27] Maselli and Peters,[28] and Rajagopalan et al.[29]

Light gases yields and selectivities are higher in CAT-SC than in CAT-LC. This difference can be attributed to a larger influence, in the case of CAT-SC, of gas oil cracking (primary reaction).[14] Also the CAT-SC catalyst produces more gasoline than the CAT-LC catalyst, contributing as a result toward higher levels of light gases via gasoline overcracking. For instance, the selectivity of light gases obtained at 510 °C and 7 s using CAT-SC and CAT-LC is 24.9% and 21.3% respectively.

The coke selectivity obtained using both types of catalysts varies considerably, with the selectivity attained using CAT-SC being lower than that obtained using CAT-LC. For instance, the difference in coke selectivity at 7 s is 1.5%. This difference in the amount of coke formed using the two catalysts can be assigned to the diffusional constraints that exist in the zeolite pore networks. Since the CAT-SC catalyst has shorter diffusional pathways from the active sites to the crystallite outer surface, there is less opportunity for coke condensation reactions to take place. On the other hand, in the CAT-LC catalyst, with longer diffusional pathways, there is an increased chance for the larger gas oil molecules to remain in the catalyst pore network to form coke. These trends are in agreement with previous literature data presented by Maselli and Peters[28] and Rajagopalan et al.[29]

Thus, it is proven in the present study that crystallite size plays a very important role in FCC catalysts for both conversion and selectivity, especially at conditions that fall under the diffusion-controlled regime. Reducing the USY zeolite crystallite size decreases the diffusional path, which causes an increase in the vacuum gas oil-cracking rate as well as causes a reduction in the tendency of gasoline and other intermediate products to overcrack. This leads to the production of more desirable products, such as gasoline, while minimizing the production of catalyst-deactivating coke and heavy hydrocarbon fractions, such as light cycle oil.

7. Conclusions

The contributions of the present manuscript can be summarized as follows:

(a) It is shown using a CREC riser simulator unit that 0.4 μm USY zeolite crystallites provide higher accessibility to active sites and increase, as a result, catalytic cracking rates of gas oil molecules. This is particularly relevant at 510−530 °C and 3−7 s reaction times.

(b) It is also proven that reduction in crystallite size lowers the diffusive path and increases the overall gas oil cracking rate, thus favoring the formation of desired products such as gasoline and reducing the formation of undesirable species such as coke.

(c) A five-lump kinetic model including gas oil, LCO, gasoline, light gases, and coke is established using the experimental and reactivity data obtained in the 510−570 °C range and by adopting a two-step modeling and numerical regression process. The resulting model, which incorporates the effects of intracrystallite hydrocarbon molecule transport, is proven to be suitable in determining the relative importance of intrinsic kinetics and species diffusion.

d) It is found that, in the 510−530 °C range, the overall cracking rate is controlled by the highly temperature-sensitive intracrystalline gas oil transport, while in the 550−570 °C range, the overall cracking rate is dominated by a mildly temperature-sensitive intrinsic cracking rate. All of this leads to the catalyst operating under the DLT−RHT regime: diffusion controlling at lower temperatures−intrinsic reaction dominating at higher temperatures.

Acknowledgment

The authors are very appreciative for the financial support of the Natural Sciences and Engineering Research Council of Canada (NSERC), which provided a Canada Graduate Scholarship (CGS) to M.A.-S. The authors would also like to acknowledge the contribution of Imperial Oil Inc. and Nobel Akzo to this research.

Nomenclature

a_{ext} = specific external surface area (m^{-1})
C_i = concentration of lump i in the vapor phase (mol/m^3)
D_{eff} = effective diffusivity (m^2/s)
D_0 = preexponential factor for diffusion (m^2/s)
E_{app} = apparent activation energy (kJ/mol)
E_D = activation energy for diffusion (kJ/mol)
E_i = intrinsic activation energy for lump i reaction (kJ/mol)
E'_0 = intrinsic activation energy for overall primary reaction (kJ/mol)
h' = modified Thiele modulus
k_i = intrinsic kinetic constant [$m^6/(kg_{crystallite}$ mole s)] or [$m^3/(kg_{crystallite}$ s)]
k_{i0} = preexponential factor for reaction [$m^6/(kg_{crystallite}$ mole s)] or [$m^3/(kg_{crystallite}$ s)]
k'_0 = preexponential factor for overall primary reaction [$m^6/(kg_{crystallite}$ mole s)]
K_i = adsorption constant for lump i [m^3/(kg of catalyst)]
L = USY zeolite crystal size (μm)
MW_i = molecular weight of lump i (kg/mol)
n = reaction order
r = radial coordinate
r_i = kinetic rate of consumption/formation of lump i [mol/($kg_{crystallite}$ s)]
t = reaction time (s)
T = reactor temperature (K)
T_0 = average temperature of experiments (813.15 K)
V = volume of the riser simulator (m^3)
W_{cr} = mass of catalyst (kg)
W_{hc} = total mass of hydrocarbons inside the riser (kg)
y_i = mass fraction of lump i in the vapor phase
$y_{i,pred}$ = mass fraction of lump i in the vapor phase predicted by kinetic model
X_E = mass of coke produced per mass of crystallite ($kg_{coke}/kg_{crystallite}$)
X'_E = mass of coke produced per mass of gas oil injected ($kg_{coke}/kg_{gas\ oil}$)

Greek Symbols

φ_{int} = intrinsic catalyst activity decay function
η_{ss} = effectiveness factor
ρ_{cr} = density of the USY zeolite crystallite (kg/m^3)
ν_i = stoichiometric coefficient for lump i calculated as MW_A/MW_i
λ = deactivation parameter, RC model

Subscripts

A = gas oil lump
B = light cycle oil lump

C = gasoline lump
D = light gases lump
E = coke

Abbreviations

CAT-LC = catalyst prepared with large zeolite crystallites
CAT-SC = catalyst prepared with small zeolite crystallites
CFL = confidence limit
C/O = catalyst-to-oil ratio ($kg_{catalyst}/kg_{gas\ oil}$)
LCO = light cycle oil
VGO = vacuum gas oil

Literature Cited

(1) Rabo, J. A. Future Opportunities in Zeolite Science and Technology. *Appl. Catal., A* **2002**, *229*, 7−10.

(2) Marcilly, C. Present Status and Future Trends in Catalysis for Refining and Petrochemicals. *J. Catal*. **2003**, *216*, 47−62.

(3) Tonetto, G.; Atias, J. A.; de Lasa, H. FCC Catalysts with Different Zeolite Crystallite Sizes: Acidity, Structural Properties and Reactivity. *Appl. Catal., A* **2004**, *270*, 9−25.

(4) Williams, B. A.; Babittz, S. M.; Miller, J. T.; Snurr, R. Q.; Kung, H. H. The Role of Acid Strength and Pore Diffusion in the Enhanced Cracking Activity of Steamed Y Zeolites. *Appl. Catal., A* **1999**, *177*, 161−175.

(5) Magee, J.; Letzsch, W. S. Fluid Cracking Catalyst Performance and Development Now and in the Future. In *Fluid Catalytic Cracking III: Materials and Processes*; American Chemical Society: Washington, DC, 1994.

(6) Al-Khattaf, S.; de Lasa, H. Activity and Selectivity of Fluidized Catalytic Cracking Catalysts in a Riser Simulator: The Role of Y-Zeolite Crystal Size. *Ind. Eng. Chem. Res*. **1999**, *38*, 1350−1356.

(7) Cerqueira, H. S.; Ayrault, P.; Datka, J.; Guisnet, M. Influence of Coke on the Acid Properties of a USHY Zeolite. *Microporous Mesoporous Mater*. **2000**, *38*, 197−205.

(8) Moustafa, T. M.; Froment, G. F. Kinetic Modeling of Coke Formation and Deactivation in the Catalytic Cracking of Vacuum Gas Oil. *Ind. Eng. Chem. Res.* **2003**, *42*, 14−25.

(9) Ancheyta-Juarez, J.; Lopez-Isunza, F.; Aguilar-Rodriguez, E. 5-Lump Kinetic Model for Gas Oil Catalytic Cracking. *Appl. Catal., A* **1999**, *177*, 227−235.

(10) Hagelberg, P.; Eilos, I.; Hiltunen, J.; Lipiäinene, K.; Niemi, V. M.; Aittamaa, J.; Krause, A. O. I. Kinetics of Catalytic Cracking with Short Contact Times. *Appl. Catal., A* **2002**, *223*, 73−84.

(11) Ancheyta-Juarez, J.; Lopez-Isunza, F.; Aguilar-Rodriguez, E.; Moreno-Mayorga, J. C. A Strategy for Kinetic Parameter Estimation in the Fluid Catalytic Cracking Process. *Ind. Eng. Chem. Res.* **1997**, *36* (12), 5170−5174.

(12) Lee, S.-L.; Chen, Y.-W.; Huang, T.-N.; Pan, W.-Y. Four-Lump Kinetic Model for Fluid Catalytic Cracking Process. *Can. J. Chem. Eng.* **1989**, *67*, 615−619.

(13) Al-Khattaf, S.; Atias, J. A.; Jarosch, K.; de Lasa, H. I. Diffusion and Catalytic Cracking of 1,3,5-Tri-iso-propyl-benzene in FCC Catalysts. *Chem. Eng. Sci.* **2002**, *57*, 4909−4920.

(14) Al-Khattaf, S.; de Lasa, H. Diffusion and Reactivity of Gas Oil in FCC Catalysts. *Can. J. Chem. Eng.* **2001**, *79*, 341−348.

(15) Dewachtere, N. V.; Santaella, F.; Froment, G. F. Application of a Single-Event Kinetic Model in the Simulation of an Industrial Riser Reactor for the Catalytic Cracking of Vacuum Gas Oil. *Chem. Eng. Sci.* **1999**, *54*, 3653−3660.

(16) Christensen, G.; Apelian, M. R.; Hickey, K. J.; Jaffe, S. B. Future Directions in Modelling of the FCC Process: An Emphasis on Product Quality. *Chem. Eng. Sci.* **1999**, *54*, 2753−2764.

(17) Oliveira, L.; Biscaia, E. Catalytic Cracking Kinetic Models. Parameter Estimation and Model Evaluation. *Ind. Eng. Chem. Res.* **1989**, *28*, 264−271.

(18) Ginsburg, J. M.; Pekediz, A.; de Lasa, H. I. The CREC Fluidized Riser Simulator. Characterization of Mixing Patterns. *Int. J. Chem. React. Eng.* **2003**, *1* (A-52), 1−12.

(19) de Lasa, H. I. Riser Simulator for catalytic cracking studies. U.S. Patent 5,102,628, 1991.

(20) Atias, J. A.; Tonetto, G.; de Lasa, H. I. Catalytic Conversion of 1,2,4-Trimethylbenzene in a CREC Riser Simulator. A Heterogeneous model with Adsorption and Reaction Phenomena. *Ind. Eng. Chem. Res.* **2003**, *42*, 4162−4173.

(21) Atias, J. A.; de Lasa, H. Adsorption and Catalytic Reaction in FCC Catalysts using a Novel Fluidized CREC Riser Simulator. *Chem. Eng. Sci.* **2004**, *59*, 5663−5669.

(22) Van Landeghem, F.; Nevicato, D.; Pitault, I.; Forissier, M.; Turlier, P.; Derouin, C.; Bernard, J. R. Fluid Catalytic Cracking: Modelling of an Industrial Riser. *Appl. Catal., A* **1996**, *138*, 381−405.

(23) Froment, G. F.; Bischoff, K. B. *Chemical Reactor Analysis and Design*, 2nd ed.; New York: Wiley, 1979.

(24) Ruthven, D. M. *Principles of Adsorption and Adsorption Processes*; John Wiley: New York, 1984.

(25) Atias, J. A.; de Lasa, H. Adsorption, Diffusion and Reaction Phenomenon on FCC Catalysts in the CREC Riser Simulator. *Ind. Eng. Chem. Res.* **2004**, *43*, 4709−4720.

(26) Ruthven, D. M.; Kaul, B. K. Adsorption of *n*-Hexane and Intermediate Molecular Weight Aromatic Hydrocarbons on LaY Zeolite. *Ind. Eng. Chem. Res.* **1996**, *35*, 2060−2064.

(27) Camblor, M. A.; Corma, A.; Martinez, F.; Mocholi, F. A.; Perez Pariente, J. Catalytic Cracking of Gas Oil. Benefits in Activity and Selectivity of Small Y-Zeolite Crystallites Stabilized by a Higher Silicon-to-Aluminum Ratio by Synthesis. *Appl. Catal.* **1989**, *55*, 65−74.

(28) Maselli, J.; Peters, A. Preparation and Properties of Fluid Catalytic Catalysts for Residual Oil Conversion. *Catal. Rev. Sci. Eng.* **1984**, *26*, 525−559.

(29) Rajagopalan, K.; Peters, A. W.; Edwards, G. C. Influence of Zeolite Particle Size on Selectivity During Fluid Catalytic Cracking. *Appl. Catal.* **1986**, *23*, 69−80.

Received for review June 10, 2005
Revised manuscript received November 25, 2005
Accepted December 1, 2005

IE050683X